A study of ternary Cu2SnS3 and Cu3SnS4 thin films prepared by sulfurizing stacked metal precursors — Source link ↗

Paulo Fernandes, Paulo Fernandes, Pedro M. P. Salomé, A. F. da Cunha

Institutions: University of Aveiro, Instituto Superior de Engenharia do Porto

Published on: 02 Jun 2010 - Journal of Physics D (IOP Publishing)

Topics: Tetragonal crystal system, Orthorhombic crystal system, Band gap, Electron backscatter diffraction and Energy-dispersive X-ray spectroscopy

Related papers:

- Thin film solar cells based on the ternary compound Cu2SnS3

- Raman analysis of monoclinic Cu2SnS3 thin films

- Cu2SnS3 and Cu4SnS4 Thin Films via Chemical Deposition for Photovoltaic Application

- Structural and optical properties of Cu2SnS3 sprayed thin films

- Non-toxic, earth-abundant 2% efficient Cu2SnS3 solar cell based on tetragonal films direct-coated from single metal-organic precursor solution

A study of ternary Cu2SnS3 and Cu3SnS4 thin films prepared by sulfurizing stacked metal precursors

P A Fernandes, P M P Salomé, a F da Cunha

Study of Ternary Cu_2SnS_3 and Cu_3SnS_4 Thin Films Prepared by Sulfurizing Stacked Metal Precursors

P.A. Fernandes[1,2,*], P.M.P. Salomé[1,a] and A.F. da Cunha[1,b]

[1]I3N, Departamento de Física, Universidade de Aveiro, Campus Universitário de Santiago, 3810-193 Aveiro, Portugal

[2]Departamento de Física, Instituto Superior de Engenharia do Porto, Instituto Politécnico do Porto, Rua Dr. António Bernardino de Almeida, 431, 4200-072 Porto, Portugal

[a] psalome@ua.pt

[b] antonio.cunha@ua.pt

[*] Corresponding author, pafernandes@ua.pt

Abstract:

Thin film Cu_2SnS_3 and Cu_3SnS_4 were grown by sulfurization of dc-magnetron sputtered Sn-Cu metallic precursors in a S_2 atmosphere. Different maximum sulfurization temperatures were tested which allowed the study of the Cu_2SnS_3 phase changes. For a temperature of 350 ºC the films were constituted by tetragonal (I-42m) Cu_2SnS_3. The films sulfurized at a maximum temperature of 400 ºC presented a cubic (F-43m) Cu_2SnS_3 phase. Increasing the temperature up to 520 ºC, the Sn content of the layer lowered and orthorhombic (Pmn21) Cu_3SnS_4 was formed. The phase identification and structural analysis was performed using X-ray Diffraction (XRD) and Electron Back-Scattered Diffraction (EBSD) analysis. Raman scattering analysis was also performed and the comparison with XRD and EBSD data allowed the assignment of peaks at 336 cm^{-1} and 351 cm^{-1} for tetragonal Cu_2SnS_3, 303 cm^{-1} and 355 cm^{-1} for cubic Cu_2SnS_3, and 318 cm^{-1}, 348 cm^{-1} and 295 cm^{-1} for the Cu_3SnS_4 phase. Compositional analysis was done using Energy Dispersive Spectroscopy (EDS) and Induced Coupled Plasma (ICP) analysis. Scanning Electron Microscopy (SEM) was used to study the morphology of the layers. The transmittance and reflectance measurements permitted the estimation the absorbance and the band gap. These ternary compounds present a high absorbance value close to 10^4 cm^{-1}. The estimated band gap energy was 1.35 eV for tetragonal (I-42m) Cu_2SnS_3, 0.96 eV for cubic (F-43m) Cu_2SnS_3 and 1.60 eV for orthorhombic (Pmn21) Cu_3SnS_4. Hot Point Probe was used for the determination of the semiconductor conductivity type. The results show that all samples are p-type semiconductor. Four Point Probe was used to obtain the resistivity of these samples. The resistivity for tetragonal Cu_2SnS_3, cubic Cu_2SnS_3 and orthorhombic (Pmn21) Cu_3SnS_4 are 4.59×10^{-2} Ω·cm, 1.26×10^{-2} Ω·cm, 7.40×10^{-4} Ω·cm, respectively.

1. Introduction

The search for materials that can overcome some difficulties present in $CuIn_{1-x}Ga_xSe_2$ (CIGS) based solar cells pointed to a new family of absorber compounds like Cu_2ZnSnS_4 (CZTS). Cheaper and non toxic materials are two of the most relevant advantages comparing with the CIGS absorbers. The maximum efficiency attained so far for CZTS based solar cells is 6.7 % [1] which is a modest value if compared with CIGS, 19.9 % [2]. Due to the increasing number of research group that have been focussing their attention to this compound it is expectable that this efficiency will increase further in the near future. Despite these advantages the CZTS shows a complex structure and requires very controlled growth conditions. If this process starts with metallic precursors, intermediate binary and ternary sulphides are formed [3,4]. These compounds will remain after the end of the growth process if the composition and the sulfurization conditions are carefully controlled. Among these ternary sulphides, Cu_2SnS_3 and Cu_3SnS_4 are the most relevant compounds. The facts above suggest the investigation of the fundamental properties of these compounds and the exploration of potential photovoltaic applications.

Few works on these compounds were reported. B. Li *et al* [5] used a solvothermal process to grow nanocrystalline Cu_2SnS_3 with a triclinic structure. M. Onoda *et al* [6] characterized Cu_2SnS_3 with monoclinic structure prepared by conventional solid-state reaction. The study of fundamental properties of tetragonal Cu_2SnS_3 and rhombohedral $Cu_4Sn_7S_{16}$ bulk crystals were done by X. Chen *et al* [7]. These compounds were grown by conventional solid-state reaction. Nanostructures, such as nanotubes and nanorods, were grown and characterized by H. Hu *et al* [8] and Y. Xiong *et al* [9], respectively. Both works used solvothermal growth routes and the chalcogenide compounds were Cu_3SnS_4 with the tetragonal structure. Cu_2SnS_3 and Cu_3SnS_4 thin films were deposited using a spray-pyrolysis technique by M. Bouaziz *et al* [10, 11]. The structural characterization showed that the Cu_2SnS_3 compound had a cubic structure and the Cu_3SnS_4 had a tetragonal structure. They also estimated a band gap of 1.15 eV and 1.35 eV for Cu_2SnS_3 and Cu_3SnS_4, respectively. These results are based on the absorption spectra which presented values near 1.0×10^4 cm^{-1}. These values present good perspectives for photovoltaic applications.

The aim of this work is to assess the potential of the ternary chalcogenide compounds, Cu_2SnS_3 and Cu_3SnS_4 (CTS), to be used as solar cell absorbers. Here we report the results of the growth and characterization of those ternary chalcogenide compounds obtained by sulfurization of dc-magnetron sputtered metallic precursors. This method presents the advantage of being easily adaptable to a manufacturing environment since sputtering is widely used in industry and the annealing temperatures applied in the sulfurization process are low compared with others technologies and materials. The fact that this method uses metallic precursors can also be considered an advantage due to the use of simpler and hence cheaper sputtering targets.

A study of the properties of these materials focusing mostly on those more relevant to judge their potential as a cell absorber layer has been performed and the results are reported here. Among others, the optical properties that are relevant for this study are the absorption coefficient and band gap energy. The semiconductor conductivity type and resistivity are the electrical parameters that were presented in this work. A compositional and structural analysis was performed to identify and characterize the compounds that are grown. The influence of the maximum sulfurization temperature on the crystallization process is also investigated.

The compositional analysis was done by EDS and ICP. The structural study was performed using XRD and EBSD. The samples were also characterized using Raman spectroscopy. The morphology of the layers was studied using SEM. The analysis of the optical transmission and reflectivity measurements allowed the estimation of the absorption coefficient and the band gap energy. The conductivity type was determined by Hot Point Probe and the resistivity was measured by 4-Point Probe.

2. Experimental details

2.1. Sample preparation

The method used in this work can be divided in two stages [4]. First, a sequential deposition of the metallic precursor layers is performed by dc magnetron sputtering. The second stage is the formation of the CZTS layer by sulfurization of the precursors.

The sample preparation process begins with the substrate cleaning, a 3x3 cm^2 SLG, with successive ultrasound baths of acetone/alcohol/deionised water. This step ends with substrate being dried with a N_2 flow. The base pressure of the sputtering system was set to be 6×10^{-6} mbar. The metallic precursors were deposited sequentially using dc-magnetron sputtering. The deposition order used was /Sn/Cu. All depositions were done under an Ar atmosphere, an operating pressure of 2×10^{-3} mbar and power densities of 0.16 Wcm^{-2} and 0.11 Wcm^{-2} for Cu and Sn, respectively. The distance between the target and the sample was set to be equal to 8 cm. The purity of the targets was 5N for Cu and 4N for Sn. In situ thickness' monitoring was performed with a quartz crystal monitor.

The crystal formation was performed in a tubular furnace in a N_2 + S_2 vapour atmosphere at a constant working pressure of 5.5×10^{-1} mbar and a N_2 flow rate of 40 ml/min. The sulphur pellets with purity 5N, were evaporated at 130 ℃ in a temperature controlled quartz tube source. The furnace temperature increased at 10 ℃/min. Different maximum sulfurization temperatures were set to study its effect on the properties of the films with the following values: 350 ℃, 400 ℃ and 520 ℃. These temperatures were kept constant during 10 min and then the system was set to cool down at a rate of 5 ℃/min down to a temperature of 200 ℃. After that, the system is left to cool down naturally. These profiles are presented in figure 1.
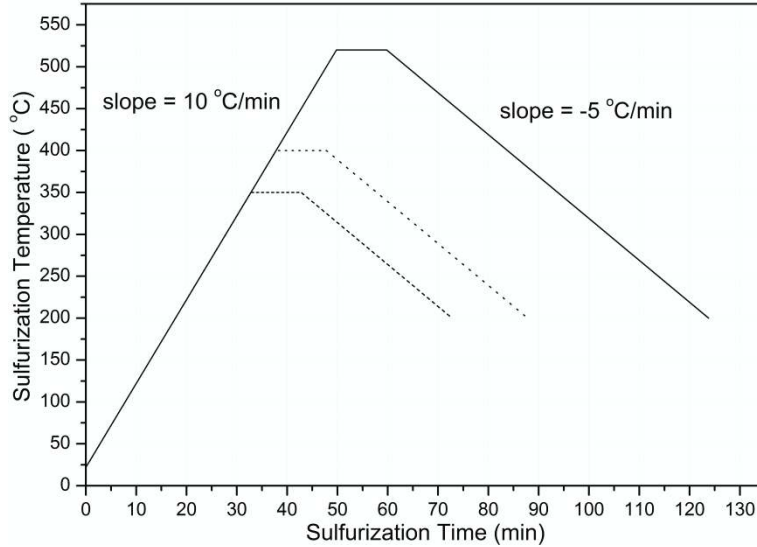

Figure 1. Sulfurization temperature profiles.

In order to eliminate unwanted phases that form during the CTS crystallization process, a KCN chemical treatment was applied to the samples [12]. For this procedure a solution of KCN at 10% w/w was prepared. The samples were, sequentially, submitted to the KCN bath, a solution of alcohol/deionised water at 50% vol/vol and finally deionised water. Each step had a duration of 2 min. Finally, all samples were dried with a N_2 gas flux.

2.2. Sample characterization

A Dektak 150 step profiler was used to measure the thickness of individual metallic precursors and the final CTS layer thicknesses. In situ thickness monitoring was done using a quartz crystal based system. X-ray diffraction analysis was performed with a PHILIPS PW 3710 system equipped with a Cu-Kα source (wavelength λ=1.54060Å) and the generator settings were 50mA, 40kV. A Hitachi Su70 with a Rontec EDS was used for compositional analysis with setting of 25 kV and 30 μA. EBSD measurements were done with a FEI Quanta 400FEG ESEM device equipped with an EDAX Genesis X4M system. Raman scattering measurements have been performed in the backscattering configuration and the excitation laser line used was

488 nm. The Jobin-Yvon T64000 Raman spectrometer was equipped with an Olympus microscope with a 100x magnification lens. It focused the laser beam down to a spot size of 1μm in diameter. This equipment has a resolution of 1 cm^{-1}. Optical measurements were done using a Shimadzu UV3600 spectrophotometer equipped with an integrating sphere. The ICP equipment was a Jobin-Yvon Activa-M system. Hot point probe analysis was performed for majority carrier identification. Resistivity measurements were done using a 4-Point Probe apparatus.

The sample naming scheme uses the letter C followed by the maximum sulfurization temperature.

3. Results and Discussion

3.1. Compositional analysis

All metallic precursors' composition was set to be slightly Cu poor for Cu_2SnS_3. The reason for using Cu poor composition is related to the fact that some loss in Sn is expected during the sulfurization process. This loss is mainly in the form of tin sulphide, SnS, form. Table 1 presents the results of the EDS and ICP measurements for the precursor as well as for the final CTS layers. It shows that the EDS results for precursors' ratio are close 2.0. This value is slightly overestimated due to the fact that precursors had a layered structure with Cu on top. These results confirmed the loss of Sn. The ratio [Cu]/[Sn] increases significantly as noted from sample C350 and C400 to C520. The ratio [S]/Metal indicates that the sulfurization process was complete. ICP compositional analysis pointed to a higher Cu content, which explains the formation of binary Cu sulphide, $Cu_{2-x}S$. These results are similar to those obtained in the growth of quaternary compound CZTS [13]. Table 1 also shows the thickness measurements for individual precursor and final sulfurized layer. It can be seen that the overall thickness change from the precursors to the CTS more than doubles for samples C350 and C400. This is explained by the lower density of the CTS than the average density of the precursors. For C520, the loss of Sn increases as well the formation of $Cu_{2-x}S$ phases. Higher material elimination occurs by KCN etching and this justifies a smaller increase in the final sample thickness.

Table 1. Atomic ratios from EDS and ICP measurements, thickness of individual metallic layers and final CTS layers.

Sample		EDS		ICP	Thickness (nm)		
		[Cu]/[Sn]	[S]/Metal	[Cu]/[Sn]	Cu	Sn	Total
C350	precursors	2.1	-	-	150	250	400
	sulfurized	2.3	1.1	2.6	-	-	850
C400	precursors	2.0	-	-	150	250	400
	sulfurized	2.1	1.0	2.6	-	-	930

C520	*precursors*	2.1	-	-	185	310	495
	sulfurized	3.1	1.1	3.2	-	-	850

3.2. Structural results

The structural analysis was performed using the XRD and EBDS techniques. Figure 2 and figure 3 show the results of XRD analysis for the three tested maximum sulfurization temperatures. In figure 2, the assignment of the phases was done using the International Centre for Diffraction Data (ICDD) database [14]. Traces of the $Cu_{2-x}S$ were also detected. This figure shows that for sulfurization temperatures of 350 ºC, the predominant phase is Cu_2SnS_3 with a tetragonal (I-42m) structure. Starting with the same precursors, the final result changed to a cubic (F-43m) structure if the sulfurization temperature rises to 400 ºC. Further temperature increase, to 520 ºC, showed the formation of a higher Cu content compound, Cu_3SnS_4 with Orthorhombic (Pmn21) structure. This result is expectable due to the sulfurization conditions. At this temperature and pressure losses of Sn in the sulphide form (SnS) are relevant.
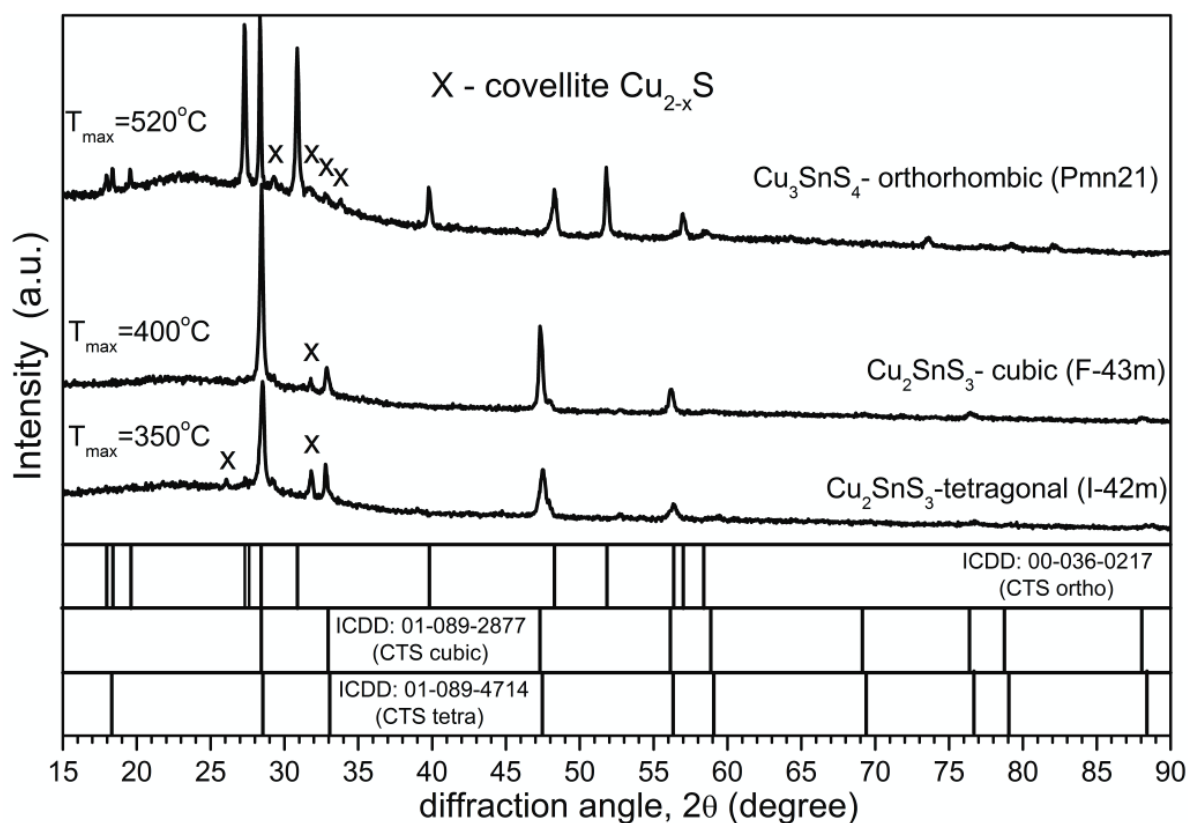

Figure 2. XRD spectra for samples sulfurized at 350 ºC, 400 ºC and 520 ºC. The phase assignment were done using ICDD database [14].

Figure 3 shows detailed spectra of the three samples at diffraction angles, 2θ, around 28.5º, 47.5º and 56.5º. The phase assignment and crystallites orientation were performed using the

ICDD database [14]. Despite the fact that cubic and tetragonal phases of Cu_2SnS_3 present peaks close to each other, the detailed analysis shown allow a clear assignment. It can be seen in the detailed XRD spectrum, for Cu_3SnS_4 compound at 2θ close to 28.5º, that a deviation from the ICDD database value. This fact may be related to the presence of strain in the sample.
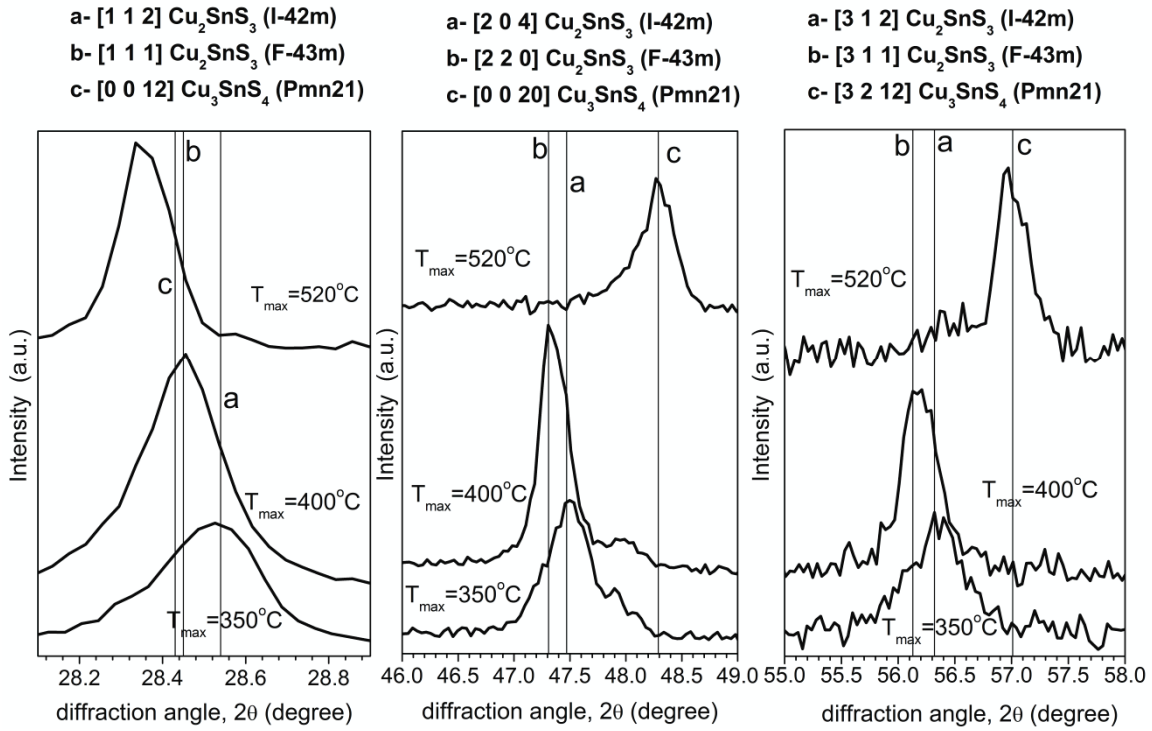

Figure 3. Detailed XRD spectra at diffraction angles, 2θ, around 28.5º, 47.5º and 56.5º, for samples sulfurized at 350 ºC, 400 ºC and 520 ºC. The phases and orientations assignment were done using ICDD database.

Using the data provided by XRD analysis we present in table 2 the lattice parameters estimation for the three compounds.

Table 2. Lattice parameters estimation for the samples under study prepared at different sulfurization temperatures using the data provided by XRD analysis and ICDD references.

Sample/Chem. Form./structure/ SPGR	ICDD ref	max sulf temp (ºC)	2θ	d (Å)	Miller Ind.	a (Å)	b (Å)	c (Å)
C350/Cu_2SnS_3/ Tetrag./I-42m	01-089-4714	350	28.58	3.12	(1 1 2)	5.412	-	10.810
			47.55	1.91	(2 0 4)			
C400/Cu_2SnS_3/ Cubic/F-43m	01-089-2877	400	28.45	3.14	(1 1 1)	5.434	-	-
C520/Cu_3SnS_4/ Orthor./Pmn21	00-036-0217	520	27.31	3.27	(2 0 0)	6.532	7.506	37.762
			28.36	3.15	(0 0 12)			
			56.98	1.62	(3 2 12)			

The level of preferential texturing for the samples C350, C400 and C520 is presented in table 3, table 4 and table 5, respectively. These tables compare the intensity ratios of the major peaks of the reference powder (4th column) with those of the samples (6th column) under study. The parameter Δ is the difference between the previous ratios. Table 3 shows that for Tetragonal (I-42m) Cu_2SnS_3 the preferential growth orientation is (1 1 2), with a diffraction angle, 2θ, equal to 28.57°. Table 4 presents the results for Cubic (F-43m) Cu_2SnS_3 and for that compound the preferential growth orientation is (1 1 1), with a diffraction angle, 2θ, equal to 28.45°. For Orthorhombic (Pmn21) Cu_3SnS_4 the preferential growth orientation is shown in table 5 and is (0 0 12) with a diffraction angle, 2θ, equal to 28.43°.

Table 3. Preferential texturing estimation for Tetragonal (I-42m) Cu_2SnS_3 - sample C350. Reference powder data used was provided by ICDD database [14].

Sample C350 : Tetragonal (I-42m) Cu_2SnS_3							
Reference				Sample			
2θ	Rel Int	h k l	I[1 1 2] / I[h k l]	2θ	Rel Int (%)	I[1 1 2] / I[h k l]	Δ
28.5398	**999**	**1 1 2**	**1.0**	**28.5656**	**100**	**1.0**	**0.0**
33.0703	132	2 0 0	7.6	33.1398	4.75	21.1	13.5
47.4725	459	2 0 4	2.2	47.507	44.17	2.3	0.1
56.3246	277	3 1 2	3.6	56.3369	12.34	8.1	4.5
76.6807	76	3 1 6	13.1	76.8577	1.74	57.5	44.3

Table 4. Preferential texturing estimation for Cubic (F-43m) Cu_2SnS_3 - sample C350. Reference powder data used was provided by ICDD database [14].

Sample C400 : Cubic (F-43m) Cu_2SnS_3							
Reference				Sample			
2θ	Rel Int	h k l	I[1 1 1] / I[h k l]	2θ	Rel Int (%)	I[1 1 1] / I[h k l]	Δ
28.4467	**999**	**1 1 1**	**1.0**	**28.4435**	**100**	**1.0**	**0.0**
32.9638	136	2 0 0	7.3	32.9654	6.73	14.9	7.5
47.3104	477	2 2 0	2.1	47.2854	45.56	2.2	0.1
56.1314	297	3 1 1	3.4	56.078	11.68	8.6	5.2
76.3896	87	3 3 1	11.5	76.3553	3.04	32.9	21.4
88.047	88	4 2 2	11.4	88.013	1.71	58.5	47.1

Table 5. Preferential texturing estimation for Orthorhombic (Pmn21) Cu_3SnS_4 - sample C520. Reference powder data used was provided by ICDD database [14].

Sample C520 : Orthorhombic (Pmn21) Cu_3SnS_4	
Reference	Sample

2θ	Rel Int	h k l	I[200] / I[h k l]	2θ	Rel Int (%)	I[200] / I[h k l]	Δ
27.318	100	2 0 0	1.0	27.3115	97.32	1.0	0.0
28.429	**75**	**0 0 12**	**1.3**	**28.3607**	**100**	**1.0**	**-0.4**
30.895	100	1 2 6	1.0	30.8747	86.92	1.1	0.1
48.294	80	0 0 20	1.3	48.303	25.72	3.8	2.5
51.847	50	2 0 18	2.0	51.7807	39.09	2.5	0.5

Table 6. Full width half maximum and crystallite size estimation considering the 3 major growth orientation planes for the samples C350, C400 and C520.

Sample C350 : Tetragonal (I-42m) Cu_2SnS_3				
Peak Pos. (deg., 2θ)	FWHM (deg., 2θ)	FWHM (deg., 2θ) corrected	$<L>$ (nm)	Size (nm)
28.58	0.30	0.14	62	83
Sample C400 : Cubic (F-43m) Cu_2SnS_3				
Peak Pos. (degree , 2θ)	FWHM (degree, 2θ)	FWHM (degree, 2θ) corrected	$<L>$ (nm)	Size (nm)
28.46	0.21	0.08	102	135
Sample C520 : Orthorhombic (Pmn21) Cu_3SnS_4				
Peak Pos. (degree , 2θ)	FWHM (degree, 2θ)	FWHM (degree, 2θ) corrected	$<L>$ (nm)	Size (nm)
28.34	0.16	0.05	172	229

Table 6 presents the results for the Full Width Half Maximum (FWHM) for the most intense peak of the XRD spectrum for each sample. The experimental points were fitted with a Gaussian curve. The estimated FWHM is corrected to account for the 0.12 degree resolution of the diffractometer. The estimation of the crystallite length, $<L>$, is performed according to the Scherrer's equation [15]. This table shows, for C350, a crystallite size of 83 nm. An increase in the crystallite size was obtained for sample C400, which presented the value 135 nm. As expected, C520 presented the highest value, which is 229 nm.

The structural analysis was complemented with EBSD. This technique was used for phase detection and orientation planes assignment. The reference used was also the ICDD database [14]. Due to the fact that this method is more localized than the XRD technique several spots have been analysed in each sample. Figure 4 shows an electron diffraction pattern for sample C350. It can be seen that for this sample the best match was achieved for Tetragonal (I-42m) Cu_2SnS_3. Figure 5 presents similar results for sample C400. This analysis confirmed the results obtained with the XRD technique that is identification of the Cubic (F-43m) Cu_2SnS_3. Figure 6 shows the EBSD results for sample C520. For this sample the phase assignment was Orthorhombic (Pnma) Cu_4SnS_4. This result did not confirm the XRD analysis which obtained a high match score for Orthorhombic (Pmn21) Cu_3SnS_4. The composition analysis with both EDS and ICP methods, points out that the compound present in this sample is Orthorhombic (Pmn21) Cu_3SnS_4. Note that for Orthorhombic (Pnma) Cu_4SnS_4 the composition ratios [Cu]/[Sn] must be close to 4.0, which is not the case.

Figure 4. Electron diffraction pattern for the sample sulfurized at 350 ºC (C350). The phases and orientations assignment were done using the ICDD database [14].

Figure 5. Electron diffraction pattern for the sample sulfurized at 400 ºC (C400). The phases and orientations assignment were done using the ICDD database [14].

Figure 6. Electron diffraction pattern for the sample sulfurized at 520 ºC (C520). The phases and orientations assignment were done using the ICDD database [14].

The Raman spectroscopy results are presented in figure 7. For the maximum sulfurization temperature of 350 ºC, C350, the Raman spectra show peaks at 336-337 cm^{-1} and 351 cm^{-1}. According to the XRD analysis these peaks are attributed to Tetragonal (I-42m) Cu_2SnS_3. Making the same correspondence for sample C400 its Raman spectrum corresponds to Cubic (F-43m) Cu_2SnS_3. The main peaks for this phase are 303 cm^{-1} and 355 cm^{-1}. The sample C520 presents peaks at 295 cm^{-1}, 318 cm^{-1} and 348 cm^{-1}, which are assigned to Orthorhombic (Pmn21) Cu_3SnS_4. No published Raman data was found for these ternary phases. These results also show the presence of $Cu_{2-x}S$ with the characteristic Raman peak at 475 cm^{-1} [4]. Another feature that can be observed with this result is the crystallinity of the compounds. The presence of a lower signal to noise ratio in the Raman spectrum of sample C350 allows the conclusion that this sample is more amorphous than the other two samples. Given the crystallite sizes estimated above, shown in table 6, no significant contributions to the Raman peak positions due to quantum confinement are expected.
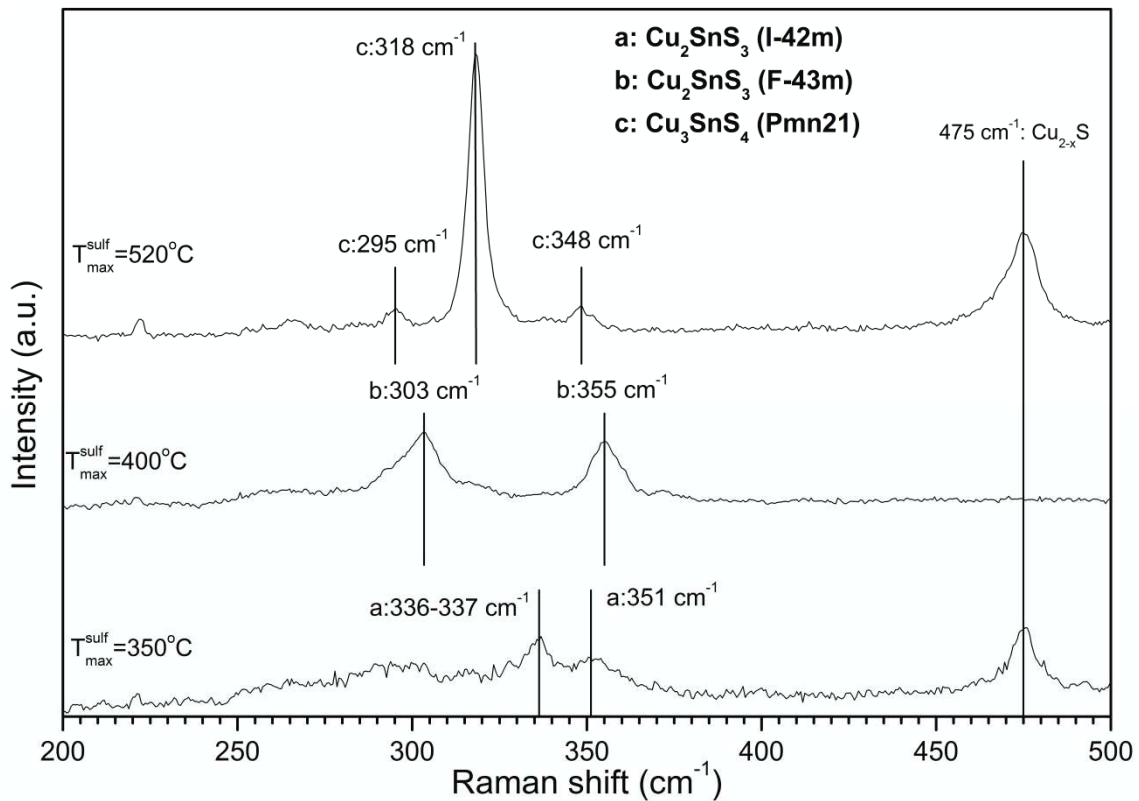

Figure 7. Raman spectra for the sample sulfurized at 350 ºC, 400 ºC and 520 ºC.

3.4 Morphological results

The morphology of the samples has been characterized through SEM, shown in figure 8. Micrograph 8-a) shows the surface of C350 sample. We can see that this sample

presents a rough surface. Using this image, XRD and Raman results we can say that this layer has a poor crystalline quality. Micrograph 8-b), corresponding to C400, shows a more compact film, some sparse large grains and a high surface roughness. The FWHM values of XRD and Raman peaks point to a slight improvement of the crystalline properties. Micrograph 8-c) shows the surface of the sample C520. It is clear that an improvement in Cu_3SnS_4 crystallinity is achieved though with a different crystal structure, namely orthorhombic. This statement is also supported by both XRD and Raman results. This film still presents some roughness and sparse voids. All these three micrographs show the points selected for the EBSD analysis referred in section 3.2 (figures 4 - 6).
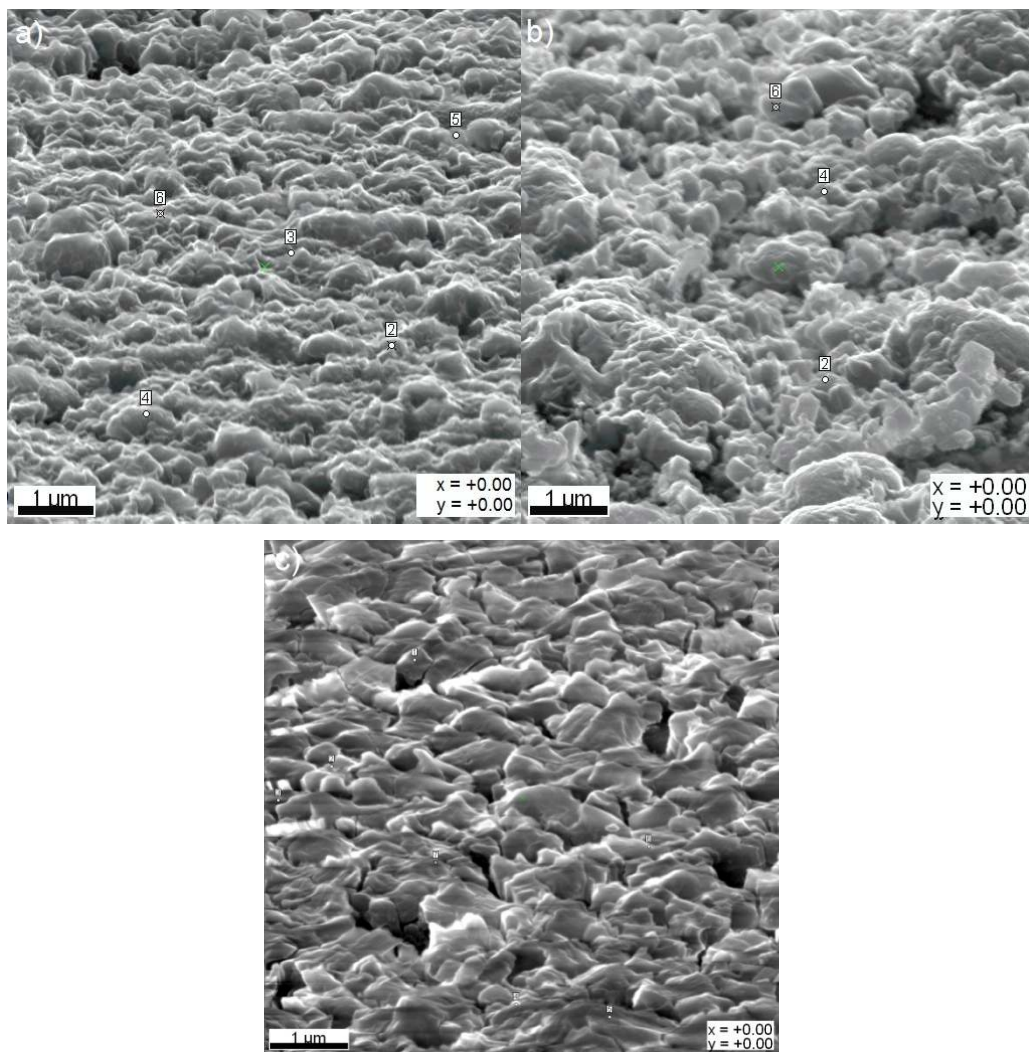

Figure 8. Surface SEM micrographs of CTS samples: a) C350, b) C400, c) C520. These micrographs also show the points selected for the EBSD analysis referred in section 3.2.

3.5 Optical results and band gap energy estimation

The results of transmission and reflectivity measurements are shown in figure 9. These graphs show that for all he samples the reflectance has a very small spectral dependence. The transmittance results shows that for samples sulfurized at temperatures of 350 ℃ a peaks is achieved at a wavelength close to 1050 nm and for temperatures of 400 ℃ the peak shifts to higher wavelength values, close to 1400 nm. The sample C520 reaches its maximum transmittance value, 26 %, at wavelength close to 750 nm and seems to stabilize at 15 % for have a smaller than 550 nm.
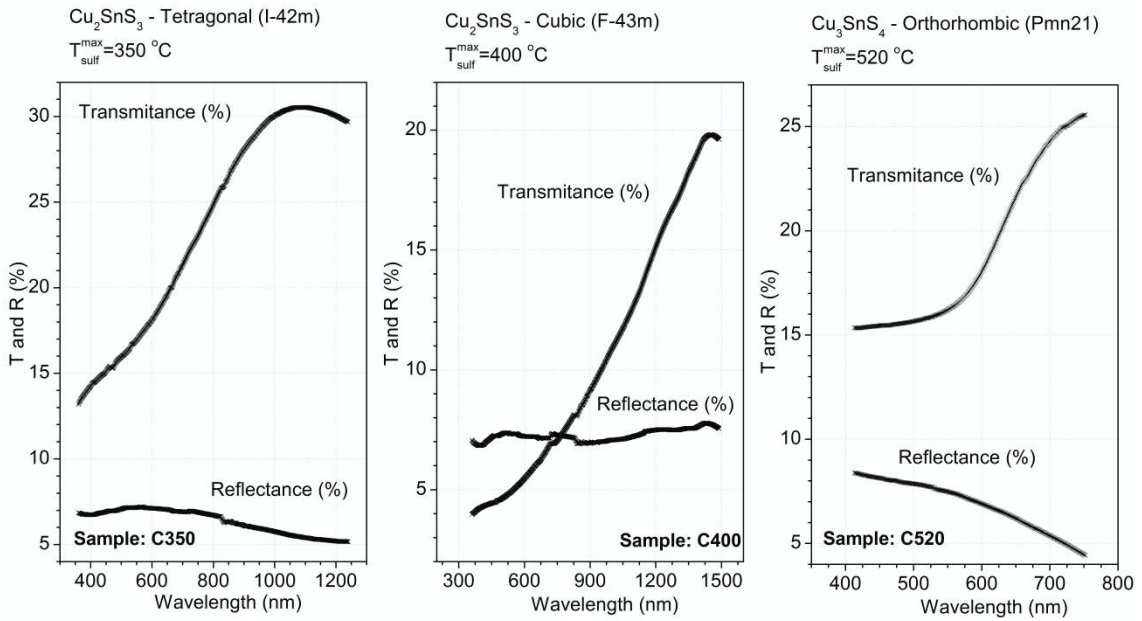

Figure 9. Transmission and reflectivity measurement results of CTS samples C350, C400 and C520.

Figure 10 shows the optical absorption coefficient, $\alpha(\lambda)$, which is estimated using the data presented in figure 9, *i e*, the transmittance measurements, $T(\lambda)$, and reflectance measurements, $R(\lambda)$, in equation 1 [16]. The required thicknesses of the layers, t, are shown in table 1.

$$\alpha(\lambda) = \frac{1}{t} \ln\left[\frac{1 - R(\lambda)^2}{T(\lambda)}\right] \tag{1}$$

Figure 10 shows high optical absorption coefficient for all the samples, above 1.2×10^4 cm^{-1}. These values are suitable for thin films solar cell applications. This figure also shows optical absorption coefficient saturation for sample C400 and C520 at photon energy close to 2.2 eV. This behaviour is not observed for sample C350.
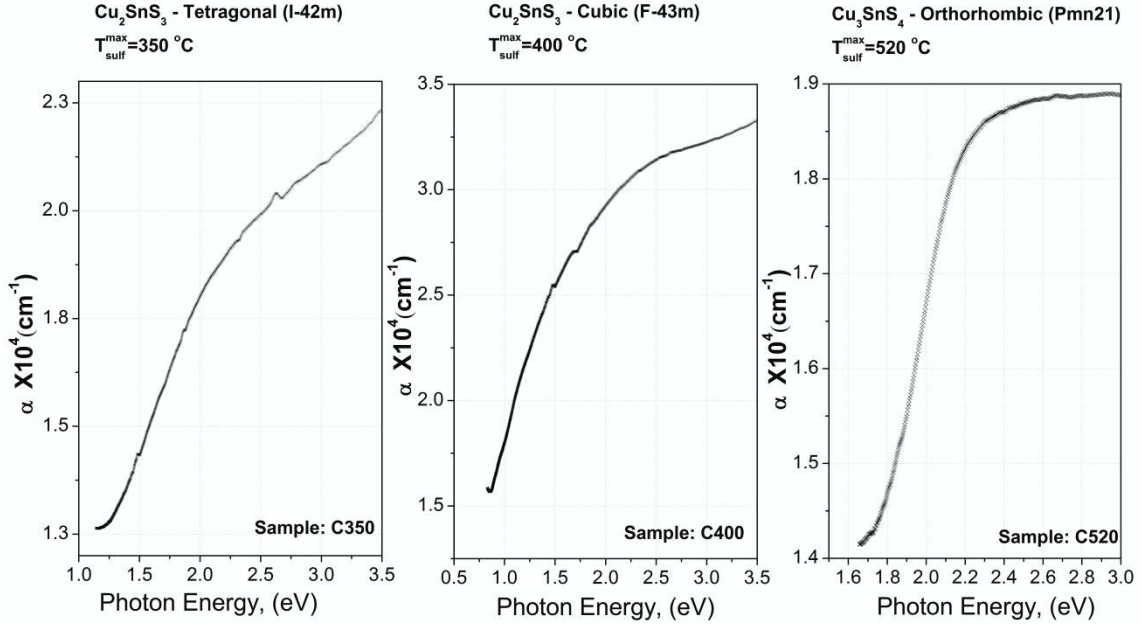
Figure 10. Optical absorption coefficient, $\alpha(\lambda)$, for CTS samples C350, C400 and C520.

Next, considering a direct-allowed optical transition in nature, n equal to 1/2, in equation 2 [16]:

$$\alpha(\lambda) = \frac{A(h\upsilon - E_g)^n}{h\upsilon}$$

(2)

where A is a constant and n defines the nature of the transition. The band gap photon energy estimation is performed extrapolating the linear region of the plot $(\alpha h\upsilon)^2$ versus $h\upsilon$ to the horizontal axis and consider the intersecting point. In figure 11 we show the band gap estimations for samples C350, C400 and C520. For C350 the band gap is 1.35 eV. To the best of our knowledge a value for the band gap energy of Tetragonal (I-42m) CTS has not been reported before. It also suggests possible photovoltaic applications. Cubic (F-43m) Cu_2SnS_3 shows a band gap of 0.96 eV. The value estimated for this compound is lower, 1.15 eV, than the band gap energy value obtained in the work done by M. Bouaziz *et al* [10]. The sample C520, with petrukite structure, shows a band gap of 1.60 eV. This value has not been reported before. To avoid the influence of the $Cu_{2-x}S$, with band gaps varying from 1.3 eV to 2.3 eV [17], all these samples were etched with KCN.
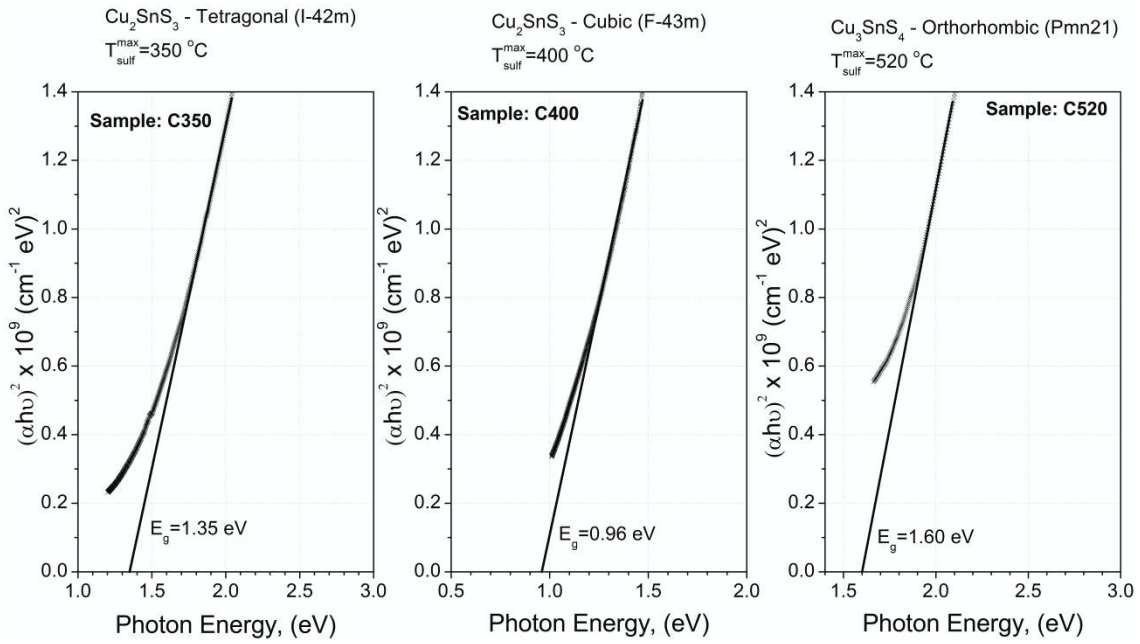
Figure 11. Band gap energy estimation of the CTS samples: C350, C400 and C520.

3.6 Electrical results

Hot point probe analysis was performed for majority carrier identification and all the samples showed a p-type semiconductor nature. Table 7 shows the results of the sheet resistance and resistivity of the samples. The thicknesses of the layers used for the resistivity estimation are shown in table 1. As shown in table 7, sample C520 presents a resistivity that is 2 orders of magnitude smaller than samples C350 and C400. This fact may be related to a higher Cu content in the sample.

Table 7. Sheet resistance and resistivity results for samples C350, C400 and C520.

Sample	Sheet resistance (Ω)	Resistivity ($\Omega \cdot$cm)
C350	540	4.59×10^{-2}
C400	135	1.26×10^{-2}
C520	8.7	7.40×10^{-4}

4. Conclusions

This work describes a method to grow ternary sulphides, Cu_2SnS_3 and Cu_3SnS_4, via the sulfurization of stacked metallic precursors. The procedure described can easily be adapted to an industrial environment due to the fact that it uses well known deposition techniques like dc-magnetron sputtering and low annealing temperatures for the crystallization process. The fact

that it uses elemental metallic precursors can constitute an advantage since no preliminary compound synthesis is required.

The structural, compositional, morphological and optical characterization was also performed.

For lower sulfurization temperatures, 350 ºC, tetragonal (I-42m) Cu_2SnS_3 forms. This compound has Raman peaks at 336-337 cm^{-1} and 351 cm^{-1} and a band gap energy of 1.35 eV. Structural analysis shows lattice parameters of 5.412 Å and 10.810 Å. For this sample, a (1 1 2) preferential growth orientation plane has been observed.

Higher temperatures result in the formation of cubic (F-43m) Cu_2SnS_3 if Sn content does decrease. This phase presents Raman scattering peaks at 303 cm^{-1} and 355 cm^{-1} and a band gap energy of 0.96 eV. The lattice parameter obtained is a = 5.434 Å. The preferential growth orientation plane is (1 1 1).

Increasing further the maximum sulfurization temperature, to 520 ºC, increases the evaporation of the binary sulphide, SnS. This fact lowers the content of Sn promoting the growth of orthorhombic Pmn21 Cu_3SnS_4. This compound presents an intense Raman peak at 318 cm^{-1} and two lower ones at 295 cm^{-1} and 348 cm^{-1}. The lattice parameters obtained are a = 6.532 Å, b = 7.506 Å and c = 37.762 Å. The preferential growth orientation plane is (0 0 12).

Electrical characterization shows that all the samples are p-type semiconductor and present the following resistivity: 4.59×10^{-2} Ω·cm, 1.26×10^{-2} Ω·cm and 7.40×10^{-4} Ω·cm, for C350, C400 and C520, respectively.

Some of these compounds present good perspectives for photovoltaic applications, especially the tetragonal (I-42m) Cu_2SnS_3 due to its optical and electrical properties. Further studies must be performed to support this statement.

Acknowledgements

References

[1] H. Katagiri, K. Jimbo, S. Yamada, T. Kamimura, W. S. Maw, T. Fukano, T. Ito, and T. Motohiro, *Appl. Phys. Express,* **1**, (2008), 041201.

[2] Ingrid Repins, Miguel A. Contreras, Brian Egaas, Clay DeHart, John Scharf, Craig L. Perkins, Bobby To and Rommel Noufi, *Prog. Photovolt: Res. Appl.,* **16** ,(2008), 235–239

[3] A. Weber, R. Mainz, T. Unold, S. Schorr, and H. Schock, *Phys. Stat. Sol. (c)*, **6**, (2009), 1245-1248.

[4] P.A. Fernandes, P.M.P. Salome, A.F. da Cunha, *Thin Solid Films*, **517**, (2009), 2519–2523.

[5] B. Li, Yi Xie, J. Huang, and Y. Qian*, Journal of Solid State Chemistry,* (2000), **153**, 170-173

[6] M. Onoda, X. Chen, A. Sato, and H. Wada, *Materials Research Bulletin*, **35**, (2000), 1563–1570.

[7] X. Chen, H. Wada, A. Sato, and M. Mieno, *Journal of Solid State Chemistry,***139**, (1998), 144-151

[8] H. Hu, Z. Liub, B. Yang, X. Chen, Y Qian, *Journal of Crystal Growth*, **284**, (2005), 226–234

[9] Y. Xiong, Y. Xie, G. Du, and H. Su, *Inorg. Chem., **41***, 2002, 2953-2959

[10] M. Bouaziz, M. Amlouk, S. Belgacem, *Thin Solid Films*, **517**, (2009), 2527–2530

[11] M. Bouaziz, J. Ouerfelli, M. Amlouk, and S. Belgacem, phys. stat. sol. (a), **204,** No. 10, (2007), 3354–3360

[12] P. A. Fernandes, P M P Salomé and A F da Cunha, *Semicond. Sci. Technol.*, 24, (2009), 105013

[13] Th. Friedlmeier, N. Wieser, Th.Walter, H. Dittrich, H.-W. Schock, *Proceedings of the 14th European PVSEC and Exhibition*, **p. P4B.10**, (1997).

[14] International Centre for Diffraction Data - Reference Code, 01-089-4714 (Tetragonal I-42m Cu_2SnS_3), 01-089-2877 (Cubic F-43m Cu_2SnS_3), 00-36-0217 (Orthorhombic Pmn21 Cu_3SnS_4).

[15] Kril C E and Birringer R 1998 *Phil. Mag.* A **77** 621–40

[16] I.V. Pankove, Optical Processes in Semiconductors, *Dover Inc., New York*, (1975), pp. 34–95.

[17] A. Sagade, R. Sharma, *Sensors Actuat. B - Chem.*, **133**, (2008), 135–143